I J C T A, 9(2) 2016, pp. 687-707

Bone Age Assessment Using Content-based Image Retrieval System with Discriminative Dictionary Learning

[1]Ananthi Sheshasaayee and [2*]C. Jasmine

ABSTRACT

Skeletal maturity is visually examined through the comparison of hand radiographs with an image atlas that acts as a standard reference. Most general ones are the techniques by Greulich and Pyle (GP) and Tanner & Whitehouse (TW). These methods try to do the extraction, measurement, classification of bones and the distances between the bones are affected due to the high dimensionality of the biological material and also the differences arising in the development of bone that results from age, gender in addition with ethnic origin. Content Based Image Retrieval (CBIR) yields a reliable solution without any delineation and measurement of bones. With a left hand-wrist radiograph provided as the input, the system does the estimation of the bone age by employing techniques for pre-processing, feature extraction, feature selection, Relevance Score (RS) and similarity matching. Initially a noise in the image samples is removed by using Hybrid Principal Component Analysis (HPCA). In feature extraction phase six important features such as Color histogram and color moments, Gabor Wavelets Transform (GWT), Edge direction histogram, GIST features,Adaptive Local Binary Pattern (ALBP) and epiphyseal Region Of Interest (eROI) features is extracted. Harmony Search (HS) is used as a feature selection technique for reducing the feature vector size. The features that are selected are provided as input into a Hybrid Fuzzy Neural Network (HFNN) classifier to assist in acquiring the search purpose from the user and further enhance the retrieval results. The relevance score computed features are fed into a Discriminative Dictionary Learning (DDL) classifier that yields the output as the class to whom the radiograph is grouped, again which is mapped to the bone age that is final. This system proposed assures precise and reliable Bone Age Assessment (BAA) for the ages ranging from 0-18 years for both the cases of girls and boys. Support BAA through the comparison of the epiphyses of a present case to the same kind of cases with bone age validated by CBIR. The performance of DDLsystem was assessed with the aid of parameters like precision, recall, sensitivity, specificity and accuracy.

Keywords: Content Based Image Retrieval (CBIR) system, Image Retrieval in Medical Applications (IRMA), Bone Age Assessment (BAA), Semantic gap measurement, Discriminative Dictionary Learning (DDL), feature selection, Harmony Search (HS), Hybrid Fuzzy Neural Network (HFNN).

1. INTRODUCTION

Bone Age Assessment (BAA) is a significant clinical means in the domain of paediatrics, particularly with respect to endocrino-logical issues and also growth disorders [1] or pediatric syndromes [2]. On the basis of a radiological assessment of development of certain parts of the skeleton, bone age is evaluated and then compared with the chronological age. A variance between these two values is indicative of the abnormalities seen in the skeletal development. The process is frequently utilized in managing and diagnosing the endocrine disorders and also helps to inform about the therapeutic impact of the treatment. It also shows if a patient growth is getting accelerated or reduced, in accordance of which the patient can then be provided treatment with growth hormones. BAA is globally utilized because of its simplicity, reduced radiation exposure, and the multiple ossification centers availability for the maturity evaluation. Under certain conditions, BAA may also contribute to forensic age diagnostics of adolescents and young adults [3-4].

[1] Professor & Head, PG & Research Department of Computer Science, Quaid-E-Millath Government College for Women, Chennai, Tamil Nadu, 600 002, India.

[2] Research Scholar, University of Madras, PG & Research Department of Computer Science, Quaid-E-Millath Government College for women, Chennai, Tamil Nadu, 600 002, India.

[*] Corresponding Author: *E-mail: Jasminesamraj.research@gmail.com*

Many different methods are used to assess skeletal maturity. Each method makes use of different parts of the skeleton. Clinically, the methods by Greulich and Pyle (GP) [5] or Tanner and Whitehouse (TW) [6] are applied. GP method is rapid and therefore easy to be used compared to the TW technique. In GP technique, the comparison of a left-hand wrist radiograph is done with a sequence of radiographs that are grouped in the atlas based on age and sex. The atlas pattern that appears artificially to resemble the clinical image is chosen. TW technique makes use of a comprehensive assessment of every individual bone, allocating it to one among the eight classes thus being reflective of its stage of development. This results in the description of every bone using scores. The sum of all the scores provides the assessment of the bone age. This technique offers the most robust results. In order to reduce the manual effort, several approaches using digital image processing have been published for semi-automatic measurements [7-8].

Even after keeping aside any segmentation issues, the available approaches for BAA do not at all times render credible results. While the previous efforts have been focused on the automatic Regions Of Interest (ROI) extraction [8], the presented work serves as a proof-of concept for Content Based Image Retrieval (CBIR) as an instrument for BAA. CBIR supporting Case Based Reasoning (CBR) [9] has come to attention for medical applications, particularly in radiology [9]. With the entailed Query-By-Example (QBE) approach, CBIR is a straightforward application of CBR regarding images, where similar images of previous cases are retrieved from a database in order to solve the given task for the query image.

In proposed system, not only images but also validated case information such as chronological age, ethnic origin, gender, and multiple bone age readings are collected, building an extensible set of ground truth data. The similarities are obtained by CBIR, and the radiologist is provided visually with what proposed system regards as the best correspondences in the database. For this purpose utilize an Image Retrieval in Medical Applications (IRMA) framework supporting image retrieval in large scale experiments, and validation processes [10-11]. For the specific application to BAA, specialized the framework to retrieve ROI similar to those of a given hand radiograph rather than using the global similarity between complete images as used for example in the Image CrossLanguage Evaluation Forum (CLEF) contests [12]. A similar approach has been introduced by Tanner and Gibbons, where manually extracted regions of interest from secondary digitization are compared by Fourier coefficients.

In the proposed CBIR framework for BAA method consists of five major phases: Pre-processing, feature extraction, feature selection, Relevance Score (RS) and similarity matching or classification. The noises existing in the fields of BAA are removed using Hybrid Principal Component Analysis (HPCA). All clinically used BAA methods refer to the epiphyseal area between the bones. So features extraction phase six different type of features are extracted.For extracted features dimensionalityreduction or feature selection is performed using Harmony Search (HS). Hybrid Fuzzy Neural Network (HFNN) based Relevance Score (RS) is using positive and negative examples provided by the user for improving the performance of the system. In similarity measure, the query image feature vector and database image feature vector are compared using the Discriminative Dictionary Learning (DDL). The remaining work is divided as follows: a brief explained existing methods of bone age assessment in section 2. The detailed information of proposed work is discussed in section 3. Section 4 provides the result and discussion, and at last, in section 5 explains in detail about the conclusion along with the result summarization by means of emphasis on this study and also mentions about future research.

2. RELATED WORK

Bone Age Assessment (BAA) of people unknown is one among the most significant topics of interest in the clinical process for the assessment of the biological maturity in children. BAA is carried out generally by making a comparison between an X-ray corresponding to the left hand wrist and an atlas containing known sample of bones. In the recent times, BAA has attained significant ground from both academics and medicine.

Manual techniques of BAA consume lot of time and are susceptible to variability from observer to observer. This is an inspiration for designing automated techniques of BAA. Nonetheless, there is remarkable research over the automated evaluation, though more of which is yet in the experimental stage. This section gives the taxonomy of the automated BAA methods and studies about the problems.

A retrieval system which is web-based and prototype case-based for BAA was presented by Fischer *et al.* [13]. Hand radiographs obtained from the University of Southern California (USC) database can be obtained by issuing an image-based query. Then the ten cases that are best matching for every epiphysis are then acquired by CBIR and then displayed with the details of their BAA, similarity score, and also the age estimate which is derived. The similarity is then approximated by means of cross-correlation. The data of USC image have been empowered by making a mark of the epiphyseal centers present between the metacarpals and distal phalanges. Leave-one-out experiments rendered a mean error rate of 0.99 years in addition with a standard deviation of 0.76 years when compared with the mean USC-BAA.

Fischer *et al.* [14]epiphyseal ROIs (eROIS) corresponding to a hand radiograph are then compared with earlier cases with a known age, enacting a human observer. Leaving-one-out experiments are performed on 1,102 left hand radiographs and 15,428 metacarpal and phalangeal eROIs obtained from the generally available USC hand atlas. The similarity between the eROIs is analyzed through a combination having cross-correlation, image distortion model, and Tamura texture characteristics, rendering a mean error rate of 0.97 years and a variance that is below 0.63 years.

Hum [15] proposed automated anisotropic diffusion, followed by a novel fuzzy quadruple division scheme to optimize the central segmentation algorithm, and finally the process ends with an additional quality assurance scheme. The designed segmentation framework works without demanding scarce resources such as training sets and skillful operator. The result analysis of the resultant images has shown that the designed framework is capable of separating the soft tissue and background from the hand bone with relatively high accuracy despite omitting the resources.

Zhang [16] presents a novel Computer Aided Design (CAD) development method along with continual non-discreet output for BAA. It depicted the way in which anisotropic diffusion filtration and canny edge detection applies in the segmentation of the carpal bones from the hand images. A knowledge-based model was capable of identifying every carpal bone from the objects that are segmented. The bone age was evaluated by a fuzzy logic system on the basis of the features of the carpal bone. The statistical assessment divulged the contribution provided by carpal bones in yielding information regarding resourceful growth in the case of young children who are less than 7 years old. It achieves greater accuracy and efficiency in BAA.

Zhang *et al.* [17] presented the implementation of a knowledge-based technique for entirely automated carpal bone segmentation and analysis of morphological feature. Fuzzy classification was then utilized for assessing the bone age on the basis of the chosen features. This technique has found successful application on all the cases where there is no overlapping of carpal bones. CAD results of a total of about 205 cases obtained from the digital hand atlas were assessed against the subject's chronological age in addition to the readings from two radiologists. It was observed that the carpal ROI retrieves effective information for the determination of the bone age for young children ranging from new-born to 7-year-old.

Hsieh *et al.* [18] proposed a computer-based system for the case of BAA, on the basis of the third digit; nevertheless, this system consists of the process of the extraction of the left hand from the X-ray image from both the hands over the same radiograph. This technique makes use of thresholding strategies and heuristic searches for rotating the radiograph in the stage of pre-processing. The system operates on the Phalangeal Region Of Interest (PROI) and then does the segmentation of the phalangeal bone with Gabor filters for the purpose of smoothing and canny edge detector along with the local variance techniques for getting the edge and refinement. In order to reduce the error rate, the system employed the carpal bone information for the subjects who are below 8 years making use of a fuzzy membership function.

Liu *et al.* [19] designed a computerized system for BAA making use of an artificial neural network on the basis of the two geometric features corresponding to the Radius, Ulna, and Short bones (RUS) and carpal bones. This system makes use of a big database containing samples and then the algorithm of particle swarm is applied for segmenting the bones. This method employs two classifiers for estimating the bone age: the first one is the RUS bone and the next one is the carpal bone for the samples that are of below nine years of age. This technique reveals a small standard deviation pertaining to the differences in comparison between the system and observer. One positive point with regard to this system is that it reduces the variability seen in the carpal bone-based system in comparison with the earlier systems.

Mansourvar *et al.* [20] designed an entirely automatic BAA system which utilizes compression methodologies on the basis of the histogram techniques. This approach operates on an image collection and similarity measures and exploits a Content Based Image Retrieval (CBIR) technique for the prupsoe of image processing. The system consists of a knowledge base containing 1100 hand X-ray radiographs which are classified by gender along with ethnicity. The assessment showed 0.170625 years for the error rate of the system thus demonstrating that this technique stands credible for BAA. But, the system cannot be relied for images having poor image quality or an abnormal bone structure.

Kim & Kim [21] proposed a method for BAA making use of a radiograph corresponding to the left hand in pediatric radiology. In this work used the Discrete Cosine Transform(DCT) and Linear Discriminant Analysis (LDA) over the epiphyseal parts that are segmented from a left hand radiograph. The LDA coefficients that are extracted are then compared with the features which are stored in the repository, and thereafter the bone age of the radiograph given is then estimated by making use of this proposed technique.

Mansourvar *et al.* [22] proposed a systematic strategy, which was performed in order to develop a new entirely automated technique for assessing the bone age making use of an Extreme Learning Machine (ELM) model, in depended to image segmentation. The measurement of ELM was then compared with Genetic Programming (GP) andArtificial Neural Network (ANN) for the purpose of evaluating the accuracy of the models. The results computed in terms of Root mean Square Error (RMSE), recall show that the ELM approach hails superiority over GP and ANN. In addition, the results divulged the reliability of of the techniques.

Brunk *et al.* [23] introduced an approach for the automated bone age classification obtained from hand x-ray images making use of the Discriminative Generalized Hough Transform (DGHT). For this purpose, a region, that characterizes the bone age (e.g. an epiphyseal plate), is then localized and next classified for determining the respective age. Both the steps are implemented making use of the DGHT, whereas the difference between the approaches is lying in the models that are used. The localization model is capable of localizing the target region over a vast range of age and hence is focused on the general features observed in all ages.

The above mentioned methods have some common disadvantages outdated data collection and inter- and intra-observer discrepanciescreated a necessity for a new data gathering and an non-subjective, automated BAA technique. Nonetheless, because of several factors such as the ambiguous number of bones that are appearing, non-uniformity seen in the soft tissue, low contrast existing between the bony structure and the soft tissue, automated segmentation and the identification of the boundaries of carpal bone poses an extreme challenge.

3. PROPOSED METHODOLOGY

The flow diagram of the proposed methodology for the Bone Age Assessment (BAA) by Content-Based Image Retrieval (CBIR)[24] is illustrated in Figure 1. In this proposed CBIR based BAA system views fivestages of the assessment analysis. The first stage performs the image pre-processing including the removal of noisy objects from the images. The noises existing in the fields of BAA are removed using

Hybrid Principal Component Analysis (HPCA). All clinically used BAA methods refer to the epiphyseal area between the bones. So features extraction phase six different type of features are extracted. For extracted features dimensionality reduction or feature selection is performed using Harmony Search (HS). Hybrid Fuzzy Neural Network (HFNN) based Relevance Score (RS) is using positive and negative examples provided by the user to improve the system's performance. Finally, images from the CBIR medical database, whose features fulfill the nearest match, are selected and corresponding similarity matching process done using Discriminative Dictionary Learning (DDL) method, which images are employed for assessing the ages of bone.

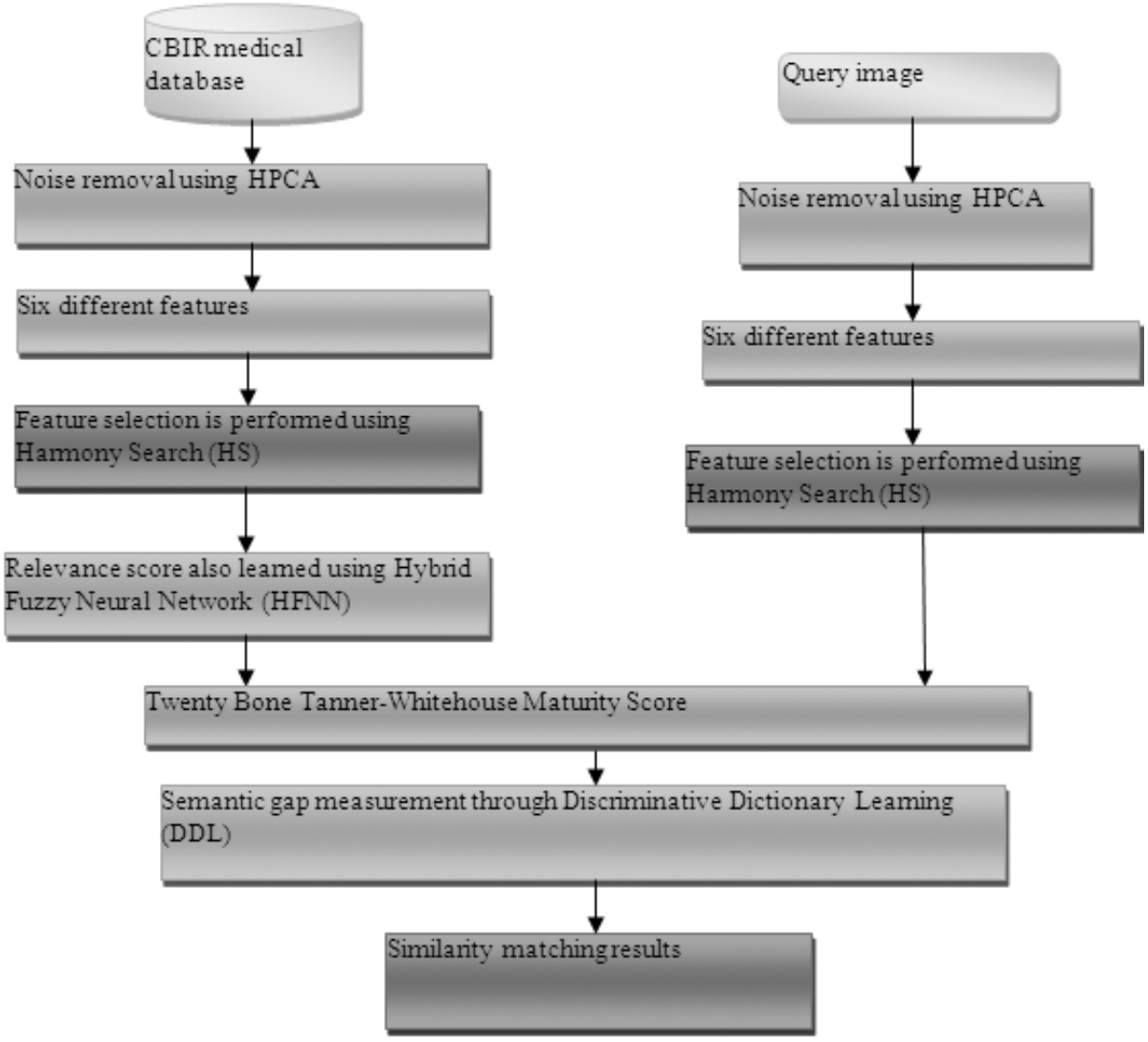

Figure 1: TheBlock diagram for Bone Age Assessment Process by using CBIR system

1.1. Pre-processing Noise removal using Hybrid PCA

A pre-processing step has been presented for the removal of background noise and for enhancing the structural characteristics. Owing to the huge differences in the size and shape of the bone complexes, Hybrid Principal Component Analysis (HPCA) technique for every kind of the bones is applied. Phalangeal epiphysal bones with a smaller dimension and a huge elongated structure had been analysed using a HPCA through by defining a Linear Discriminant Analysis (LDA) function. On the other hand, Radius / Ulna bones, with a larger size and having similar axes, are processed exploiting a set of HPCA. Inorder to prevent the border effects, pre-processing is applied tothe image before ROI extraction. The PCA noise

removal subspace is reduced based on LDA is called as hybrid PCA. Consider $X = (x_1, \ldots x_n), x \in \chi$ represents the BAA samples which is a random subset of $\mathbb{R}_n$, for every image samples pixels of the samples is indicated as $x \in P = \{ps_1, \ldots ps_m\}$. For finding W, let W refer to a unit vector ($||W|| = 1 = W^T W$) then sample X on W like as in dot product. The outcome is $x_1^T W$, $x_2^T W, \ldots x_n^T W$. The bigger the variance the higher is the data distribution. Hence 'X' was considered that its average was zero for the purpose of getting the variance.

$$\begin{aligned} Var(W, X) &= \frac{1}{n}\sum_{i=1}^{n}\left(x_i^T W\right)^2 = \frac{1}{n}\sum_{i=1}^{n}\left(W^T x_i\right)\left(x_i^T W\right) = W^T\left(\frac{1}{n}\sum_{i=1}^{n} x_i x_i^T\right)W \\ &= W^T C W \end{aligned} \tag{1}$$

C = covariance matrix. Equation(1) is giving a solution in order to find $Var(W, X1)$. The maximum value of $W^T CW$ can be got when W is a unit vector. The solution equates to $CV = VD$ is. V is a matrix in which columns are the respective Eigenvectors and D refers to a diagonal matrix having Eigen-values for BAA samples. Eigen-values are variance of W direction to BAA samples. So the principal components can be got by the Eigen-vector with big Eigen-value. This matrix is applied for multiplying with the input BAA samples and will then be utilized along with the input BAA samples. In this examination, the size of minimized BAA samples was chosen as the same as LDA for the cause as described in the section below.

LDA: Linear Discriminant Analysis (LDA) can be employed for the reduction of noise. The main concept of LDA is finding the noise subspace that had projected the BAA samples data along with the same class just nearer in comparison with the other class. Rather than getting the variance of X, here the between-class covariance and within class covariance are found.

$$S_b = \sum_k n_k (\mu_k - \mu)(\mu_k - \mu)^T \tag{2}$$

$$S_w = \sum_k \sum_{i \in k}^{n_k} (x_i - \mu_k)(x_i - \mu_k)^T \tag{3}$$

Where S_b is between-class covariance and S_w is is within-class covariance. n_k is amount of the data of the k class, μ_k is the average vector of k class and μ is average vector of entire BAA samples. In order to have the separation of the BAA samples into group, $|W^T S_b W|$ between-class variance, has to be maximized and $|W^T S_w W|$, within the class variance, must be reduced. In conclusion, it is required that the Eigenvectors and Eigen-values of $S_w^{-1} S_b$ are to be found. Hybrid PCA is a combination procedure between PCA and the LDA. The maximum variance can be computed by

$$W_{opt} = \arg\max_x \frac{|W^T[(1-\lambda)S_b + \lambda C]W|}{|W^T[(1-\eta)S_w + \eta I]W|} \tag{4}$$

(λ, η) stand for two parameters observed in the range of (0, 0) to (1, 1).

- (λ=0, η=0) the transformation minimizes to full LDA.
- (λ=1, η=1) the transformation goes back to full PCA.
- (λ=0, η=1) provides a subspace which is chiefly defined by the maximization of the scatters seen among all the classes along with reduced effort on clustering of every class.
- (λ=1, η=0) yields a subspace which chiefly preserves the most of the energy while reducing the scatter matrices of the within-classes.
- (λ=0.5, η=0.5) provides a subspace which is a compromise between LDA and PCA.

The best noise minimization can be got from this HPCA technique by means of the summation of chosen Eigen-values divided by the summation of all the Eigen-values. In this examination (λ=0, η=1) gives the most completed noise reduction. Then the features belonging to the carpal bones and the distal epiphysis of the radius bone were extracted.

4.1. Feature extraction

The methodology for the CBIR-based bone age assessment is in accordance with comparing image content from a noise removed images to earlier cases. All clinically used BAA methods refer to the epiphyseal area between the bones, so the extraction of the features from the noise removed images becomes very important. Therefore extract those areas as epiphyseal Regions Of Interest (eROIS) of each image in a standardized way. Instead of applying a query on the complete image, every eROI is used for an individual query to the database. Then most significant six categories of features are extracted in this phase. The six features are,

1. Color histogram and color moments (81 dimensions),
2. Gabor wavelets transform (120 dimensions),

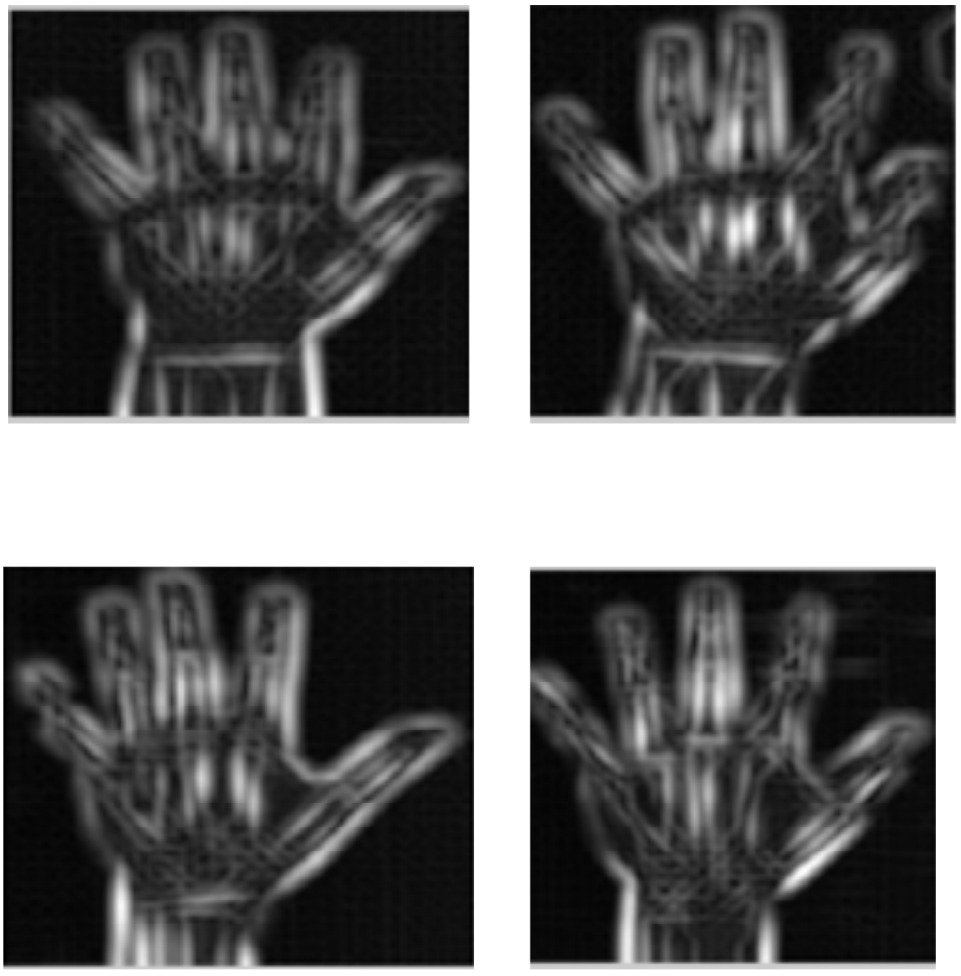

Figure 2: Gabor wavelet transform feature extraction results for all images

Gabor wavelet transform outcome of the feature extraction for the entire input image samples results are illustrated in Figure 2.

3. Edge direction histogram (37 dimensions),

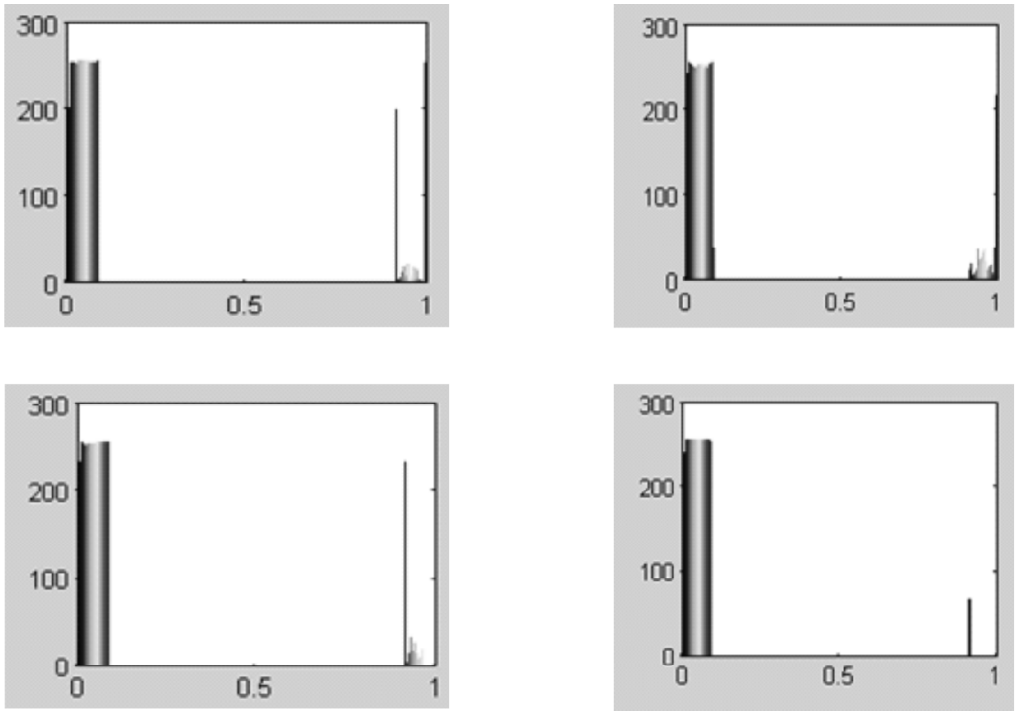

Figure 3: Edge direction histogram feature extraction results for all images

Edge histogram outcome of the feature extraction for the entire input image samples results are illustrated in Figure 3.

4. GIST features (512 dimensions),
5. Local binary pattern (59 dimensions), Adaptive Local Binary Pattern (72 dimensions)

Local Binary Pattern (LBP) evaluation from bone age assessment with respect to the texture parameters from LBP based image might render much more significant information on bones. In the LBP technique, the eight neighbor pixels for every pixel in the ROI were analyzed and an 8-bit LBP-value were calculated (Table 1). Weight positions present in the LBP weight matrix were fixed to be in perpendicular direction to bone fibers in order to get the fibers enhanced better. LBP is constructed by thresholdingneighbor pixels by means of the grayscale value of the center pixel and then having the binary matrix multiplied with the weight matrix. Weights were fixed to be in perpendicular direction to bone fibers in order to get better enhancement of the fibers.

Table 1
LBP

5	3	4
8	5	1
9	7	6

Example matrix

1	0	0
1		1
1	1	1

Thersholded binary matrix

4	2	64
16		128
8	1	32

Weights

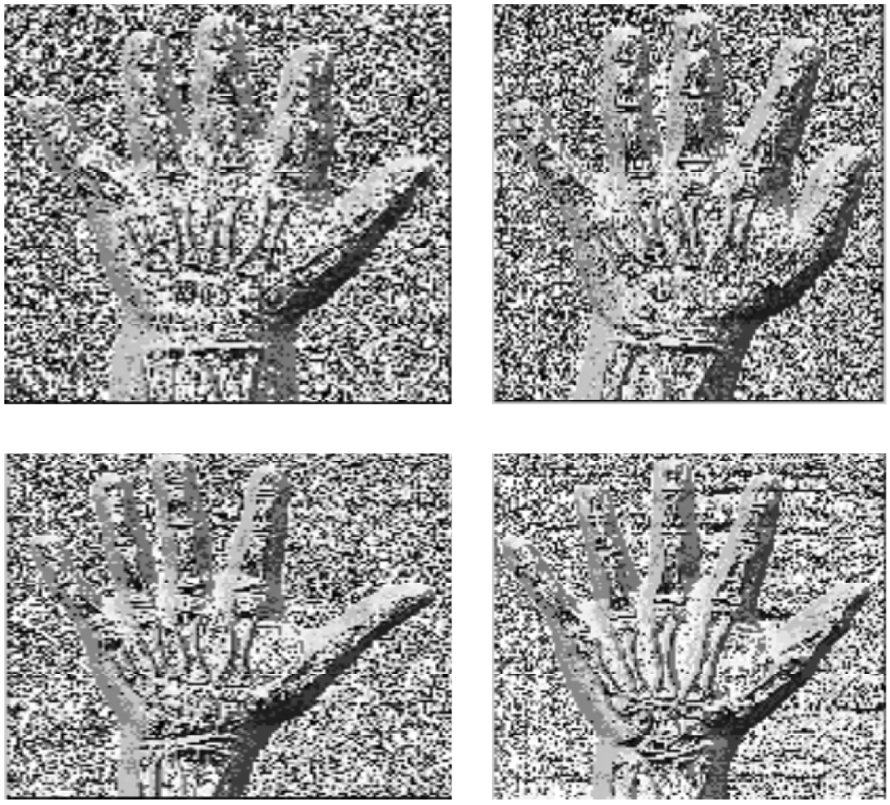

Figure 4: LBP feature extraction results for all images

LB Poutcome of the feature extraction for the entire input image samples results are illustrated in Figure 4.

Adaptive Local Binary Pattern (ALBP): In [25] is utilized the oriented standard deviation information about the the neighborhood in the step of matching for obtaining the rotation invariance. ALBP technique that takes diverse sizes of the neighbourhood into consideration for creating a distinct feature vector for the cause of rotation invariance. To this end, an Adaptive LBP (ALBP) scheme is proposed here to minimize the difference along different orientation of texture features. Specifically, this work introduces a parameter we_p so that the overall difference $|g_o - we_p * g_p|$ can be minimized. The objective function is given as follows:

$$we_p = \arg\min_{we} \left\{ \sum_{i=1}^{N} \sum_{j=1}^{M} | g_c(i,j) - we * g_p(i,j) |^2 \right\} \tag{5}$$

The Least Square Estimation (LSE) technique can be used for such an optimization and the weight we_p can be easily computed as follows:

$$we_p = \frac{\vec{g}_p^T \vec{g}_c}{\vec{g}_p^T \vec{g}_p} \tag{6}$$

where $\vec{g}_c = [g_c(1,1), g_c(1,2); ...; g_c(N,M)]$ is a column vector containing all the possible $g_c(i,j)$ image pixels and $\vec{g}_p = [g_p(1,1), g_p(1,2); ...; g_p(N,M)]$ is the corresponding vector for all $g_p(i,j)$ image pixels. Each weight we_p is then estimated along only one single orientation $2\pi p/P$ for the entire image. Finally, the ALBP is defined as:

$$ALBP_{P,R} = \sum_{p=0}^{p-1} s(g_p * we_p - g_c)2^P \quad (7)$$

Where P refers to the total number of involved neighbors and R refers to the radius of the neighborhood pixels of images. Let $\overrightarrow{we} = [we_0, we_2, ..., we_{p-1}]$ be the ALBP weight vector. ALBP weight vector is also shifted with the rotation of the image and it can align $\overrightarrow{we}$ of two different BAA image samples.

6. eROI Extraction

The first stage, i.e. the extraction of the eROIs, can be either performed fully automatically as demonstrated by semi-automatic. In the latter case, the user first defines the centers of the eROIs by clicking into them. Afterwards the rest of the eROI extraction is performed automatically by extracting oriented bounding boxes around the center coordinates. The orientation is decided by the mean of the direction of orientation of the connecting lines between the eROIcenter and the center above (if applicable) and below of the same finger. For an image of 256 pixels height, an eROI size of 25x30 pixels has proven suitable. The eROI size for larger images is chosen appropriately shown in Figure 5.

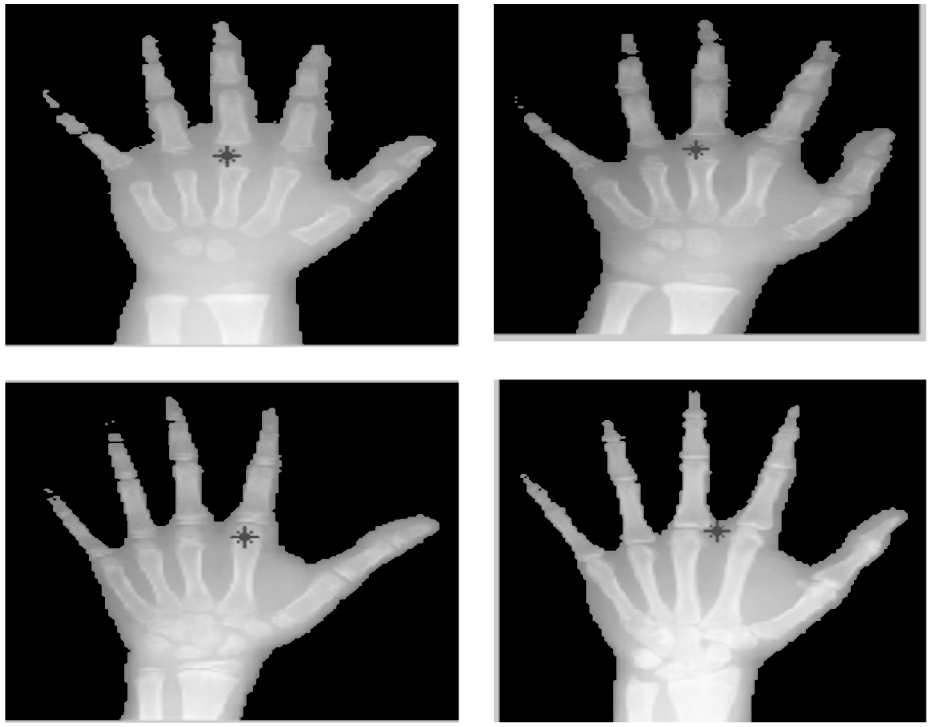

Figure 5: eROI feature extraction results for all images

These global features have been extensively employed in the previous CBIR researches. In case of local features, obtain the bag-of-visual-words features by means of two categories of descriptors:

1) SIFT descriptoradopt the Hessian-Affine interest area detector with threshold 500; and
2) SURF descriptor implements the SURF detector with threshold 500.

In case of the clustering phase, implement a forest of 16 kd-trees and look for 2,048 neighbours to accelerate the clustering process. In the end, implement the TF-IDF weighing scheme to produce the concluding bag of- visual-words representation. By means of selecting different descriptors (SIFT/SURF) and vocabulary sizes (200/1,000), completely extracted four kinds of local features: SIFT200, SIFT1000, SURF200, and SURF1000.

4.2. Feature selection utilizing Harmony Search

Feature selection eliminated the features having low discriminant power and thereby helps in reduction of the space dimensions. From the chosen carpal bone parameters, the skeletal age can be estimated by analyzing further. This system indicated the significance of making use of a multidimensional feature analysis for the case of BAA. It also pointed out that area, perimeter, ratio, number of carpal bones, local features and the global features were the vital features to be taken into consideration. These parameters along with the parameters that are extracted from the phalangeal analysis could be utilized for assessing the ages of bone. Harmony Search (HS) [26] is an evolving algorithm that is motivated by the improvisation procedure of music players. Basically, any possible feature selection solution is modelled as a harmony and each feature of the BAA images to be optimized can be seen as a musical note. The best harmony called solution is selected as the one which helps in the maximization of some optimization criterion. The Harmony Search (HS) algorithm is an interesting approach for several applications mainly because of its simplicity and low computational cost. The proposed system is using this HS for feature selection of BAA samples. The Harmony searchalgorithm comprises of few steps which is explained below:

Step 1: Initialize the problem of optimization and algorithm parameters. The Harmony search parameters required to solve the optimization problem are also specified in this step. They are: the Harmony Memory Size (HMS) = 20, the Harmony Memory Considering Rate (HMCR) = 0.9, the Pitch Adjusting Rate (PAR) is not utilized in this feature selection process. And the stopping criterion is the maximum number of iterations (T) = 5000. HMCR is parameter used to improve the solution vector.

Step 2: Initialize a Harmony Memory (HM). In this Step, the HM (feature) matrix is initialized with randomly generated BAA feature vectors with their respective score values for the objective function. Highest value of the each feature is considered as fitness value for reducing space dimensions.

Step 3: Improvise a newer harmony from HM. In this Step, a New Harmony feature vector is produced from the HM on the basis of memory considerations, pitch adjustments, and randomization (music improvisation). It is also feasible to select the new value making use of the HMCR parameter, which varies between 0 and 1 as follows: The HMCR is actually the probability of selecting one value from the historic values that are stored in the HM, and (1-HMCR) is defined as the probability of selecting randomly one possible value that is not restricted to those which are stored in the HM.

Step 4: Update the HM. if the New Harmony feature vector is better in comparison to the worst harmony feature vector in the HM, include the New Harmony (feature) in HM, and afterwards remove the worst one from HM.

Step 5: If the stopping criterion is not satisfied, go to Step 3.In this Step, the HS algorithm completes when it meets the exit criterion. Else, Steps 3 and 4 are repeated for improvising a new harmony again.

4.3. Relevance score learned using Hybrid Fuzzy Neural Network (HFNN)

The main goal of relevance score learning is to selectrelevant and irrelevant medical images provided by the user to improve the BAA performance in CBIR system. For a given query, the system at first obtains a list of reduced BAA image features in accordance with predetermined similarity metrics, which are often defined as the distance between feature vectors of BAA images. Then, the user selects a set of relevant and irrelevant images for BAAfrom the images that are retrieved, and the system afterwards does the refinement of the query and does a new list of images retrieval. The key issue is how to incorporate relevant and irrelevantimage to refine the query and how to adjust the similarity measure according to the feedback. Here this proposed work uses a Hybrid Fuzzy Neural Network (HFNN) relevance scoremethod. This HFNN is a modified version of Multilayer Feedforward Neural Network (MFNN)with four different layers. There are four layers in an HFNN. The first layer is equivalent to the fuzzification with 2N neurons. Membership

functions and numbers of fuzzy variables for the inputs need be determined in this layer. The second one is similar to the fuzzy if and then rule base with neurons. The number of neurons in the second layer is set equal to the maximum number of necessary if-then rules for a given fuzzy inference system. The last two layers are functionally equivalent to defuzzification. The combination of layer 3 and 4 is simply a MFNN with neurons and single neuron. Let and be the inputs and the output denote by.

Layer 1:In this layer, the incoming feature vectors of BAA samples are the inputs to the HFNN. Here convert the feature vector values into the fuzzy value by defining appropriate membership functions. For a given feature vectors (fv), the degree of membership for each fuzzy set is expressed as:

$$\mu_N(fv) = \begin{cases} 1, & fv < \alpha_N \\ \dfrac{(\alpha_N - fv)}{\beta_N - \alpha_N} & \alpha_N \le fv \le \beta_N \\ 0, & fv > \beta_N \end{cases} \tag{8}$$

$$\mu_z(fv) = \begin{cases} 0, & fv < \alpha_z \\ \dfrac{(fv - \alpha_z)}{\beta_z - \alpha_z} & \alpha_z \le fv \le \beta_z \\ \dfrac{(\alpha_z - fv)}{\beta_z - \alpha_z} & \beta_z \le fv \le \gamma_z \\ 0, & fv > \gamma_z \end{cases} \tag{9}$$

$$\mu_p(fv) = \begin{cases} 0, & fv < \alpha_p \\ \dfrac{(fv - \alpha_p)}{\beta_p - \alpha_p} & \alpha_p \le fv \le \beta_p \\ 1, & fv > \beta_p \end{cases} \tag{10}$$

It is noted that these parameters, such as α_z, β_z and γ_z, are adjustable rather than fixed in the HFNN. There is a corresponding node for each fuzzy set. If the input domain is divided into three different fuzzy sets, there are three nodes for this input. Since there are two inputs to this HFNNand each input domain has three fuzzy sets, the total number of nodes is six. The outgoing image of each node is therefore the corresponding membership degree. This will express the outgoing images of this layer as :

$$O_i^{1a} = \mu_{a_i}(a)\,, i = 1,2,3,\ O_j^{1b} = \mu_{bj}(b)\,, j = 1,2,3 \tag{11}$$

Layer 2 :The role of this layer is to replace the fuzzy logic rule base in the fuzzy inference system. Instead of being fully interconnected to the nodes of the previous layer, each neurons in layer 2 will only receive two input feature vectors from the 1st layer, $O_i^{1\alpha}$ & O_j^{1b}. One of the advantages of HFNN is with regard to the number of neurons in 2nd layer can be determined as long as the number of fuzzy variables in each input domain is specified as follows: $O_{ij}^2 = O_i^{1a} w_{ij}^a + O_j^{1b} w_{jl}^b - O_i^{1a}.O_j^{1b} w_{jl}^b,\ i, j = 1,2,3.,$

Layer 3 :Consequently, the output of the 3rd layer is expressed by multiplying results of second layer to weight matrix (w_{ij}^k) as,

$$I_k^3 = \sum_{i=1}^{3}\sum_{j=1}^{3} w_{ij}^k O_{ij}^2 K = 1,2,3. \tag{12}$$

$$O_k^3 = f(I_k^3) \tag{13}$$

Layer 4 : Let $w_k^c = 1,2,3,$ denote the weight connecting layer 3 and layer 4, the output of HFNN is

$$z = \sum_{k=1}^{3} w_k^c O_k^3 \; k = 1,2,3. (4) \tag{14}$$

In practical implementation, bias vector is usually added in the layer 3 and layer 4 so that the HFNN is able to approximate mappings which assign nonzero relevant score to zero input images.Novel neural network architecture such as HFNN has been proposed in this work for RS, which providesapredefined similarity measure for accurate BAA.

Tanner-Whitehouse method: In order to evaluate the bone age for RS measured features the Tanner-Whitehouse method was used [6]. For this technique, 20 bones are required to be analyzed: distal radius, distal ulna, first, third and fifth metacarpals, proximal phalanges of the thumb, third and fifth fingers, middle phalanges of the third and fifth fingers, distal phalanges of the thumb, third and fifth fingers, the seventh carpal bones: capitate, hamate, triquetral, lunate, scaphoid, trapezium and trapezoid. Every bone, adheres to Tanner-Whitehouse method, was then graded into 8 or 9 stages of maturity. Staging were allocated in conformance with the rating system of the Tanner-Whitehouse technique. The epiphyseal region were staged by means of distinction existing in the size, shape, density, smoothness or thickening along the borders, thickness of epiphyseal line, the extent of fusion and capping.

4.4. Semantic gap measurement through Discriminative Dictionary Learning

Measuring the semantic gap allow us to develop retrieval systems that are able to shorten or bridge the gap. Liu *et al.* [27] introduced a method based on information theory to measure the semantic gap. They considered the mutual information between the information quality of images and the user-desired information quality of images as the measure of semantic gap, where the user-desired information computed by comparing the results of a retrieval system to the user's query; and the similarity was measured based on low-level features of images. In this section present the details of proposed Discriminative Dictionary Learning (DDL) approach for semantic gap measurement between the user query image and database images. DDL is formulated which learns a flexible nonlinear proximity function in order to enhance visual similarity search in CBIR. Consider $Y = [y_1, y_2, ..., y_N] \in \mathbb{R}^{n \times N}$ indicates the feature vector RS learning results of query image with *n*-dimensional feature description. Provided a dictionary $A = [a_1, a_2, ..., a_N] \in \mathbb{R}^{n \times k}$, in which a_i indicates the i-th dictionary atom with I_1 regularization calculates the similarity score for input RS feature vector and it is given as $[x_1, x_2, ..., x_N] \in \mathbb{R}^{k \times n}$, of the feature vector from RS, through solving the following I_1 minimization complication,

$$X^* = \arg\min_x \sum_{i=1}^{N} (\| y_i - Ax_i \|_2^2 + \gamma \| x_i \|_1) \tag{15}$$

where γ constant indicates a sparsity constraint factor and then the term $\| y_i - Ax_i \|_2^2$ indicates the reconstruction error for matching results. In order to get hold of discriminative feature vector *x* by means of the pairwise constrained dictionary the non-subjective function for dictionary creation is provided as follows:

$$< A^*, X^* > = \arg\min_{A,X} \sum_{i=1}^{N} (\left|\left|y_i - Ax_i\right|\right|_2^2 + \gamma \left|\left|x_i\right|\right|_1) + \frac{\beta}{2} \sum_{i,j=1}^{N} ||x_i - x_j||_2^2 M_{ij} \tag{16}$$

$$\arg\min_{A,X} \sum_{i=1}^{N} (\left|\left|y_i - Ax_i\right|\right|_2^2 + \gamma \left|\left|x_i\right|\right|_1) + \beta(\mathrm{Tr}(X^T X D) - \mathrm{Tr}(X^T X M)) \tag{17}$$

In which the constants γ and β manage the virtual share of the resultant terms. The first $\| y_i - Ax_i \|_2^2$ term indicates the term of reconstruction error that assesses the reconstruction error corresponding to the approximation. The second term indicates the regularization term. The last term $\| x_i \|_1$ that is fresh and proposed at this point, indicates the discrimination term referred to as 'pair- wise error feature vector' in accordance with the pairwise constraints that are encoded in matrix $M.D = diag\{d_1,...,d_N\}$ indicates a diagonal matrix where the diagonal elements are the sum of the elements of the row in M,

$$d_i = \sum_{j=1}^{N} M_{ij} \,.\, L = D - M \tag{18}$$

L Refers to the Laplacian matrix. Matrix *M* has various forms in accordance with the setbacks being taken into account. As a result, provided the sets having 'similar feature vectors from RS learning' and 'diverse feature vectors from RS learning' pairs *S* and *D*, characterize matrix *M* for encoding the (dis)similarity information as given below,

$$M_{ij} = \begin{cases} +1 \text{ if } (y_i, y_j) \in S \\ -1 \text{if } (y_i, y_j) \in D \\ 0 \text{ else} \end{cases} \tag{19}$$

The non-subjective function for the learning of a pairwise constrained dictionary *A* for query and input image feature vectors from FNN having both reconstructive and discriminative power can be given as:

$$< A^*, X^*, W^* >= \arg\min_{A,X,W} \sum_{i=1}^{N} (\left|\left|y_i - Ax_i\right|\right|_2^2 + \gamma \left|\left|x_i\right|\right|_1) + \frac{\beta}{2} \sum_{i,j=1}^{N} ||x_i - x_j||_2^2 M_{ij} + \alpha \sum_{i,j=1}^{N} ||h_i - Wx_i||_2^2 + \lambda \left|\left|W\right|\right|_2^2 \tag{20}$$

$\left|\left|h_i - Wx_i\right|\right|_2^2 + \lambda \left|\left|W\right|\right|_2^2, \left|\left|h_i - Wx_i\right|\right|_2^2$ indicates the classification query matching error, $\left|\left|W\right|\right|_2^2$ indicates the term of regularization penalty, assists in learning of an optimal linear predictive classifier $h_i = [0,0,..,1,..,0,0]^T \in \mathbb{R}^m$ refers to a label vector related to a feature vectors results from HFNN learning, where non-zero position represents the class label of y_i.

5. EXPERIMENTATION RESULTS

The assessment for extended query based image retrieval system was realized within the content based Image Retrieval with Medical Image (IRMA) framework. An online presentation for medical image retrieval in accordance with the IRMA framework. Medical CBIR can be done in a demonstration mode by means of the images within the IRMA system. A snapshot of the input image with X-ray skull and hand bone image is illustrated Figure.2. The image retrieval results are illustrated in Figure 2. It was traced with the assistance of Google image search for "X-ray skull" and hand images, and obtained from the University of Illinois at Chicago, College of Medicine, Department of Radiology, available online at (*http://www.uic.edu/com/ uhrd/images/ Simpson_headXray.jpg*). In general, the epiphyseal regions of interest (eROI) reliably indicate the bone age (Figure. 6), especially in the range of the bone ages between 2 and 18 years [1].

In order to obtain comparable image patches for CBR, each eROI is extracted in a standardized way. The eROIcenters can be either computed fully automatically or located interactively: At first, the positions of the topmost fingertip and the top of the ulna are marked to ensure comparable scaling independent of the provided image resolution. In the next step, the centers of relevant eROIs are localized by corresponding

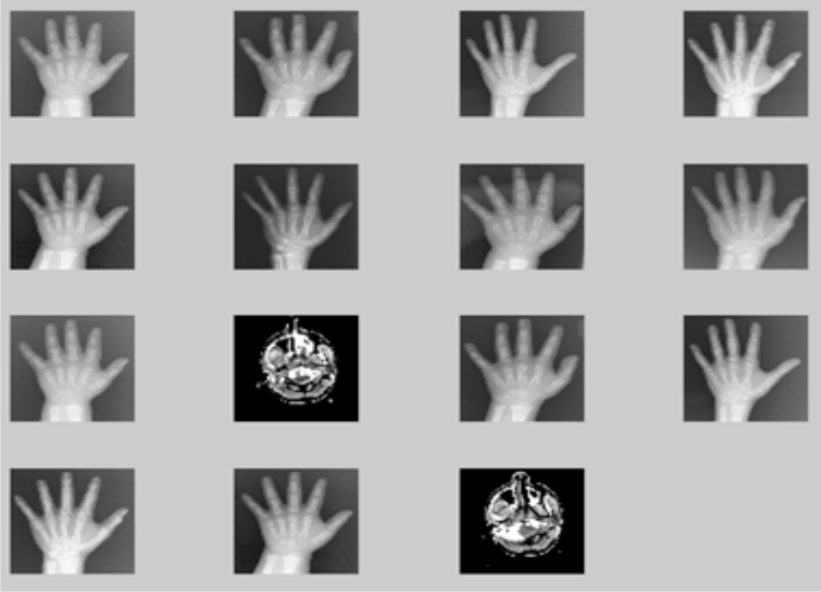

Figure 6: Successive stages of skeletal development of healthy male subjects, the radiographs have been acquired at the University Hospital Aachen, Germany

mouse clicks. Up to 19 eROIs may be used for BAA (Figure 7). In accordance with restrictions of the automatic eROI extraction algorithm, only the 14 eROIs between metacarpals and upper phalanx are used for the age estimation. In other words, eROIs 4, 8, 12, 16, and 19 are disregarded in further processing. After that, the relevance feedback learning and complete bone age determination process is performed fully automatically. Similarity matching is also performed in final stage of the work. With its fundamental flexible construction of image processing and image retrieval approaches, the IRMA framework was fine-tuned to enhance CAD in the perspective of Bone Age Assessment (BAA). In view of the fact that the IRMA system incorporation into clinical information systems can be realized by Digital Imaging and Communications in Medicine (DICOM) Hosted Applications and DICOM Structured Reporting.

MarjanMansourvar *et al.* [20] formulated a Histogram based matching (HM) to carry out CBIR for IRMA framework. In recent times, an automatic scheme combining CBIR and SVM regression has been formulated by Daniel Haak *et al.* [28]. The automatic localization of the eROIs will be enhanced by the Generalized Hough Transform (GHT) as used in [23]. The results of the experimentation of the new DDL

Figure 7: Assigned labels for the eROI positions

with IRMA framework for Spine Pathology & Image Retrieval System (SPIRS) [29] was constructed at the U. S. National Library of Medicine to retrieve x-ray image and radiographs from clinical routine image is determined with SVM [30]. BAA on hand radiographs is an expensive and time consuming process in radiology.

Table 2
Best results for individual eROIs

Ages	*Min-mean*					*Min-SD*				
	HM	*SVM*	*GHT*	*DDL-FNN*	*DDL-HFNN*	*HM*	*SVM*	*GHT*	*DDL-FNN*	*DDL-HFNN*
1	1.62	1.56	1.42	1.36	1.28	1.75	1.62	1.541	1.428	1.25
2	1.43	1.36	1.28	1.138	1.045	1.61	1.56	1.438	1.3812	1.241
3	1.12	1.08	1.101	0.96	0.89	1.28	1.23	1.18	1.08	0.984
4	1.28	1.23	1.13	1.053	1.012	1.46	1.425	1.381	1.124	1.054
5	1.38	1.32	1.24	1.38	1.24	1.23	1.187	1.085	0.918	0.854
6	1.21	1.15	1.06	1.02	0.95	1.21	1.156	1.096	0.951	0.921
7	1.3	1.26	1.21	1.18	1.021	1.15	1.09	0.963	0.9218	0.905
8	1.21	1.15	1.06	1.02	0.97	1.48	1.398	1.238	1.18	1.025
9	1.09	1.04	1.02	0.91	0.85	1.32	1.256	1.181	1.015	0.954
10	1.43	1.38	1.32	1.264	1.125	1.24	1.212	1.163	1.017	0.974
11	1.41	1.32	1.241	1.185	1.042	0.962	0.921	0.865	0.8231	0.812
12	1.43	1.39	1.361	1.215	1.145	1.43	1.381	1.238	1.1381	1.036
13	1.62	1.58	1.46	1.416	1.354	1.27	1.23	1.168	0.963	0.925
14	1.58	1.46	1.43	1.382	1.241	1.102	1.042	1.0121	0.915	0.894
15	1.26	1.18	1.06	0.935	0.904	1.57	1.52	1.4231	1.218	1.124
16	1.63	1.52	1.463	1.381	1.214	1.24	1.138	1.0814	0.9812	0.914
17	1.68	1.43	1.381	1.2861	1.158	1.63	1.581	1.4238	1.3181	1.301
18	1.38	1.36	1.248	1.182	1.124	1.31	1.236	1.1821	1.0315	0.9841

For each eROI, the observed minimum mean absolute prediction error and the minimum standard deviation are provided with the corresponding number of retrieved eROIs, *K*. The ranking provides an alternative ordering by the quality measures instead of the eROI number. The best outcomes are given in bold. To judge the prediction potential of individual eROIs, quality measures were obtained for each eROI between classification methods . The results show mean absolute error rates between 0.91 and 1.62 years and minimum standard deviations between 0.76 and 1.75 (Table 2).

4.1. Sensitivity, Specificity and accuracy

Experimentation results of the proposed IDL methods for IRMA framework for two medical images shown in the Figure 8 and Figure 9 resultsare assessed with the help of the following metrics. In medical statics commonly exploited measurements are sensitivity and specificity defined as follows:

$$Sensitivity = \frac{positive\,items\,classified\,as\,positive}{all\ positive\,items} \tag{21}$$

$$Specificity = \frac{negative\,items\,classified\,as\,negative}{all\,negative\,items} \tag{22}$$

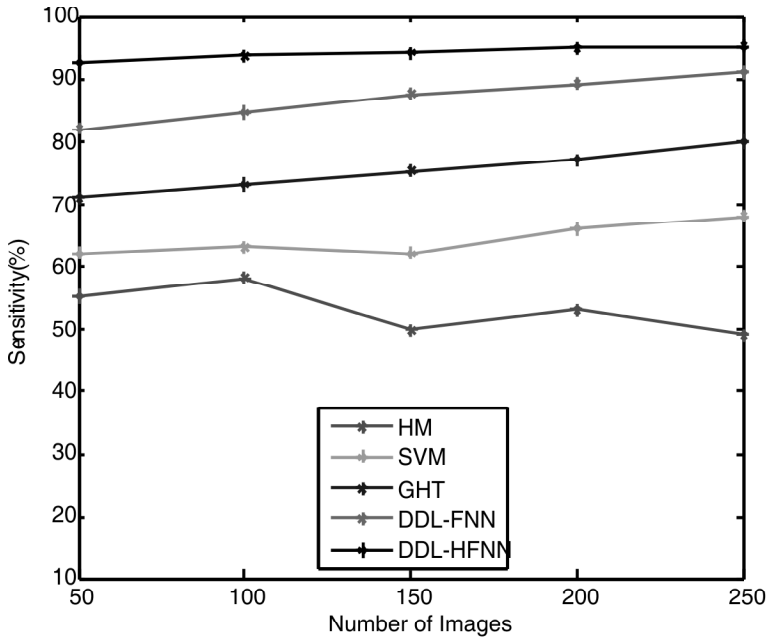

Figure 8: Sensitivity results comparison for X rays images in IRMA

The experimentation results of the proposed IDL with IRMA framework for Spine Pathology & Image Retrieval System (SPIRS) [29] was constructed at the U. S. National Library of Medicine to retrieve x-ray image and radiographs from clinical routine image is determined with SVM [31]. It demonstrates that the sensitivity results of the IDL proposed for x-ray skull images have better sensitivity in comparison with the other available approaches, in view of the aspect that it eliminates noise from x ray image samples at first prior to carrying out similarity matching, RS learning also done in the work proposed. The results are illustrated in Figure 8. The experimentation specificity results of the proposed and existing methods for clinical routine image are represented in Figure 9. It shows that the performance results of the proposed system is less since it falsely retrieve results are less.

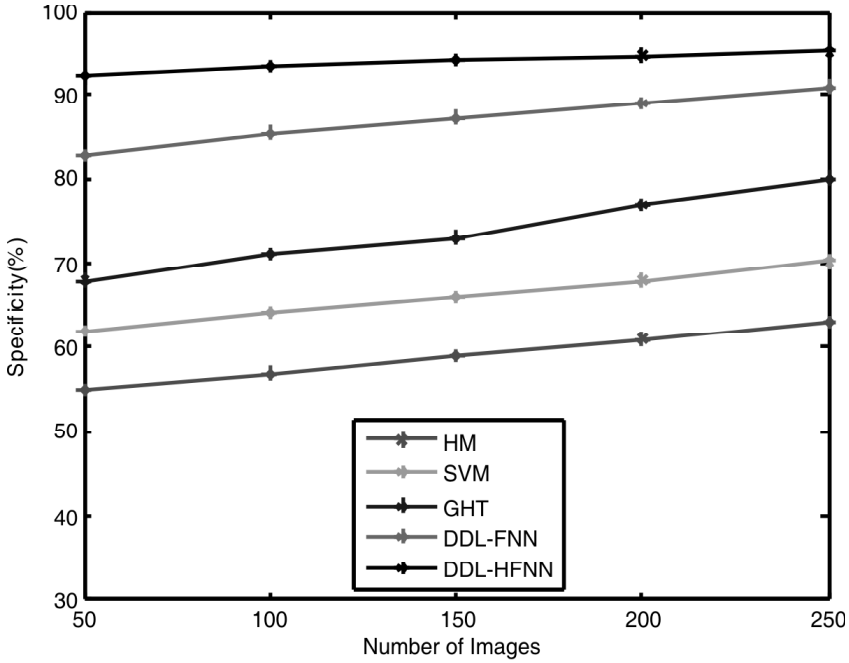

Figure 9: Specificity results comparison for X rays images in IRMA

Since several of the systems that are introduced make use of the classifications of images, accuracy is fundamentally employed to evaluate the system,

$$Accuracy = \frac{items\ classified\ correctly}{all\ items\ classified} \tag{27}$$

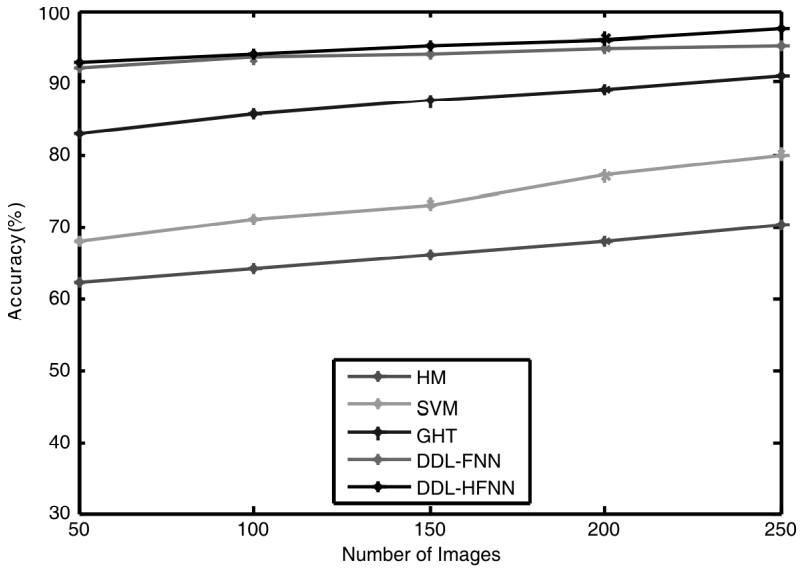

Figure 10: Classification results comparison for X rays images in IRMA

The experimentation classification results of the proposed DDL with IRMA framework for SPIRS was constructed at the U. S. National Library of Medicine to retrieve x-ray image and radiographs from clinical routine image is determined with SVM. It shows that the classification results of the proposed DDL for x-ray skull images are better than the existing approaches, as it eliminates noise from x ray image samples at first prior to carrying out performing similarity matching and then accurately performed matching for the entire image samples are illustrated in Figure 10.

Precision and Recall

It is to be noted that CBIR are not primarily being utilized for classification purpose, however for discovery of similar images or cases. This is habitually more supportive as the consultant must still have to makes a judgement on the cases retrieved and the causes for the images retrieval are frequently clear while the classification results are sometimes hard to detail and need to be explained. In order to evaluate CBIR, numerous performance evaluation measures have been available [29], here used the precision P and the recall R, and defined as follows:

$$Precision = \frac{no.relevant\ items\ retrieved}{no.items\ retrieved} \tag{23}$$

$$Recall = \frac{no.relevant\ items\ retrieved}{no.relevant\ items} \tag{24}$$

It shows that the precision and recall results of the proposed IDL-HFNN for x-ray skull images have higher than the existing methods, since it removes noise from x ray image samples initially before performing similarity matching, results of the precision values are illustrated in Figure 11.

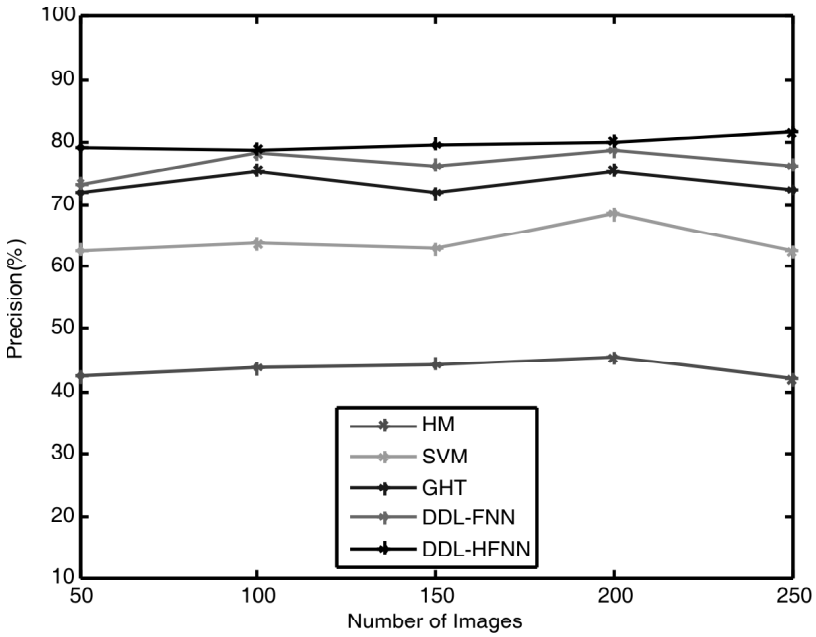

Figure 11: Precision results comparison for X rays images in IRMA

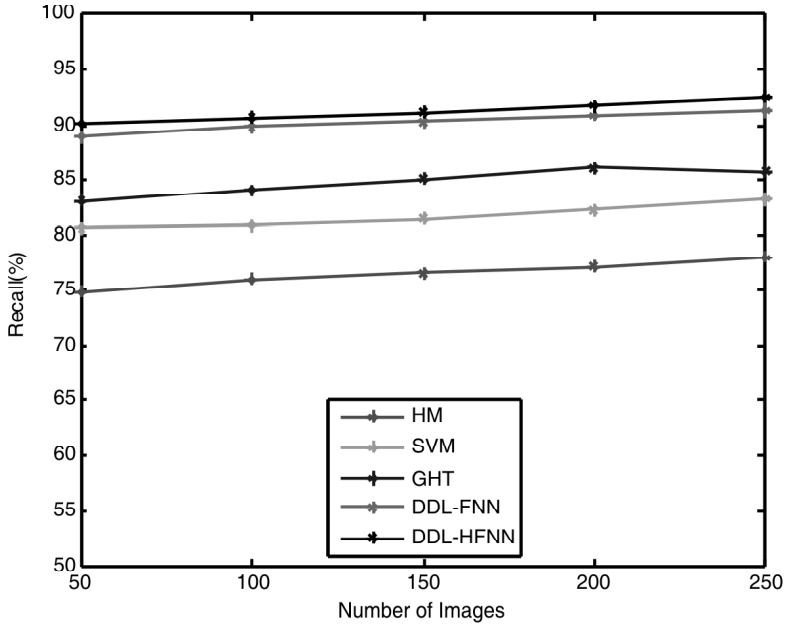

Figure 12: Recall results comparison for X rays images in IRMA

The experimentation recall results of the proposed and existing methods for clinical routine image are represented in Figure.12. It shows that the performance results of the proposed system is less since it falsely retrieve results are less.

5. CONCLUSION AND FUTURE WORK

Maturity estimation by means of radiological Bone Age Assessment (BAA) is a task done frequently by pediatric radiologists. BAA is performed usually by comparing an X-ray of left hand wrist with an atlas of known sample bones. Proposed system assists BAA through the comparison of the epiphyses of a current case with similar kind of cases with the help of bone age that is validated by Content-Based Image Retrieval (CBIR). CBIR yields a reliable solution without any delineation and measurement of bones. Noisy images

and data that is incomplete or poor contrast of few of the sections in the hand images are the critical issue for the case of automated BAA. So initially noise in the image samples is removed by using HPCA. Then feature extraction is done using feature extraction methods. BAA analysis is a crucial point for enabling the feature selections to gain a fine BAA that contains ROI processing. So feature selection is performed using Harmony Search (HS) to reduce dimension of features. The proposed Hybrid Fuzzy Neural Network (HFNN) classifier is employed from a huge amount of labelled loosely medical images feature vectors and a lesser amount of accurately labelled BAA images. In order to compute the similarity matching between query and input image samples novel Discriminative Dictionary Learning (DDL) is proposed. It is anticipated that a DDL-HFNN system would enhance the accuracy, recall, sensitivity, specificity and the precision of BAA in research practice. Future work will concentrate on improvements of the similarity computation, web site usability, and comprehensive validation.

REFERENCES

[1] V.Gilsanz, and O. Ratib Hand bone age. A Digital Atlas of Skeletal Maturity. Springer, Berlin. 2005.

[2] H.H. Thodberg, "An automated method for determination of bone age," The Journal of Clinical Endocrinology & Metabolism. Vol.94. No.7. pp.2239–2244, 2009.

[3] A.Schmeling, U. Lockemann, A. Olze, W. Reisinger, A. Fuhrmann, K. Puschel, and G. Geserick. "Forensische Altersdiagnostik bei Jugendlichen und jungen Erwachsenen." DEUTSCHES ARZTEBLATT-KOLN- 101. No. 1. pp.1007-1011, 2004.

[4] R. Schmitt, and U. Lanz, Diagnostic imaging of the hand, Thieme Publishing Group, Stuttgart. pp 148. 2008.

[5] W.W.Greulich, and S.I.Pyle, Radiographic atlas of skeletal development of hand wrist. Stanford University Press, California. 1971.

[6] J.M.Tanner, M.R.J.Healy, H. Goldstein, and N.Cameron Assessment of skeletal maturity and prediction of adult height (TW3). WB Saunders, London. 2001.

[7] A. Gertych, A.Zhang, J.Sayre et al, "Bone age assessment of children using a digital hand atlas, " Comput Med Imaging Graph. Vol.31. No.4–5. pp.322–331, 2007.

[8] H.H. Thodberg, S.Kreiborg, A.Juul, and K.D.Pedersen, "The BoneXpert method for automated determination of skeletal maturity," IEEE Trans Med Imaging. Vol.28, no. 1. pp.52–66, 2009.

[9] H. Muller, N.Michoux, D.Bandon, and A.Geissbuhler, "A review of content-based image retrieval systems in medical applications Clinical benefits and future directions," Int J Med Inform. Vol. 73, No.1. pp.1–23, 2004.

[10] E.S.Berner, and J.J. McGowan, "Use of diagnostic decision support systems in medical education," Methods Inf Med. Vol. 49. No.4. pp. 412–417, 2010.

[11] T.M.Lehmann, M.O. Güld, C. Thies, B. Fischer, K .Spitzer, D .Keysers, H. Ney, M. Kohnen, H.Schubert, and B.B. Wein, "Contentbased image retrieval in medical applications," Methods Inf Med. Vol.43. No. 4. pp.354–361, 2004.

[12] M.O. Güld, C.Thies, B.Fischer, and T.M.Lehmann, "Content-based retrieval of medical images by combining global features," Lecturer notes in computer science. Vol. 4022, pp 702–711. 2006.

[13] B. Fischer, P.Welter, R. W. Günther, and T. M. Deserno, "Web-based bone age assessment by content-based image retrieval for case-based reasoning," International journal of computer assisted radiology and surgery. Vol.7. No. 3. pp.389-399, 2012.

[14] B. Fischer, P. Welter, C. Grouls, R. W. Günther, and T. M. Deserno, "Bone age assessment by content-based image retrieval and case-based reasoning," In SPIE Medical Imaging International Society for Optics and Photonics. pp. 79630P-79630P, 2011.

[15] Y. C. Hum, Segmentation of hand bone for bone age assessment. Springer. pp.1-132. 2013.

[16] A. Zhang, A computer-aided-diagnosis (CAD) method combining phalangeal and carpal bone features for bone age assessment of children. University of Southern California, Dissertation, Biomedical engineering. pp.1-126. 2007.

[17] A. Zhang, A. Gertych, and B. J. Liu, "Automatic bone age assessment for young children from newborn to 7-year-old using carpal bones," Computerized Medical Imaging and Graphics. Vol.31. No.4. pp. 299-310, 2007.

[18] C. W. Hsieh, T. L. Jong, and C. M. Tiu, "Bone age estimation based on phalanx information with fuzzy constrain of carpals," Medical and Biological Engineering and Computing. Vol. 45. No. 3. pp. 283–295, 2007

[19] J. Liu, J. Qi, Z. Liu, Q. Ning, and X. Luo, "Automatic bone age assessment based on intelligent algorithms and comparison with TW3 method," Computerized Medical Imaging and Graphics, vol. 32, no. 8, pp. 678–684, 2008

[20] M. Mansourvar, R. G. Raj, M. A. Ismail, *et al.*, "Automated web based system for bone age assessment using histogram technique," Malaysian Journal of Computer Science. Vol. 25. No. 3. pp. 107–121, 2012.

[21] H. J. Kim, and W. Y. Kim, Computerized bone age assessment using DCT and LDA. InComputer Vision/Computer Graphics Collaboration Techniques. Springer Berlin Heidelberg. pp. 440-448. 2007.

[22] M. Mansourvar, S.Shamshirband, R. G.Raj, R. Gunalan, and I. Mazinani, "An Automated System for Skeletal Maturity Assessment by Extreme Learning Machines," PloS one. Vol.10. No. 9. pp. e0138493, 2015.

[23] M.Brunk, H. Ruppertshofen, S.Schmidt, P. Beyerlein, and H. Schramm, Bone age classification using the discriminative generalized hough transform. In BildverarbeitungfürdieMedizin. Springer Berlin Heidelberg. pp. 284-288. 2011.

[24] B. Fischer, A. Brosig, P.Welter, C.Grouls, R.W. Guenther, and T.M. Deserno, "Content-based image retrieval applied to bone age assessment," Proc SPIE 2010. Vol.7624. DOI: 10.1117/12.844392

[25] Z. Guo, "Rotation invariant texture classification using adaptive LBP with directional statistical features.' In IEEE International Conference on Image Processing (ICIP), pp.285—28, 2010.

[26] M.A. Mashinchi, W.Orgun, and Pedrycz, "A Tabu Harmony Search Based Approach to Fuzzy Linear Regression," IEEE Transactions on Fuzzy Systems. Vol.19. No.3, pp.432-448, 2011.

[27] C. Liu and G. Song, "A method of measuring the semantic gap in image retrieval: Using the information theory," in Image Analysis and Signal Processing (IASP). pp. 287–291, 2011.

[28] D.Haak, H.Simon, J.Yu, M. Harmsen, and T.M. Deserno, "Bone Age Assessment Using Support Vector Machine Regression", Bildverarbeitungfür die Medizin 2013 Informatikaktuell. pp 164-169, 2013

[29] W. Hsu, L.R. Long, and S.Antani, "SPIRS: a framework for content-based image retrieval from large biomedical databases", MEDINFO 2007: Proceedings of the 12th World Congress on Health. pp.188-192.

[30] I.F. Amaral, F.Coelho, J.F. Pinto da Costa, and J.S. Cardoso, "Hierarchical Medical Image Annotation Using SVM-based Approaches.' in Proceedings of the 10th IEEE International Conference on Information Technology and Applications in Biomedicine, 2010.

[31] H. Muller, W. Muller, D.M. Squire, S.M. Maillent, T. Pun, "Performance Evaluation in Content-Based Image Retrieval: Overview and Proposals," Elsevier Pattern Rec. Lett. Vol.22. pp.593–601, 2001.